

Excited State TBA for the $\phi_{2,1}$ perturbed $\mathcal{M}_{3,5}$ model

R. M. Ellem, V. V. Bazhanov[‡]

*Department of Theoretical Physics, RSPHysSE, IAS,
Australian National University, Canberra, ACT 0200, Australia.*

Abstract

We examine some excited state energies in the non-unitary integrable quantum field theory (IQFT) obtained from the perturbation of the minimal conformal field theory (CFT) model $\mathcal{M}_{3,5}$ by its operator $\phi_{2,1}$. Using the correspondence of this IQFT to the scaling limit of the dilute A_2 lattice model (in a particular regime) we derive the functional equations for the QFT commuting transfer matrices. These functional equations can be transformed to a closed set of TBA-like integral equations which determine the excited state energies in the finite-size system. In particular, we explicitly construct these equations for the ground state and two lowest excited states. Numerical results for the associated energy gaps are compared with those obtained by the truncated conformal space approach (TCSA).

[‡]email: Vladimir.Bazhanov@anu.edu.au

1 Introduction

The problem of calculating the excited state energies in finite volume integrable quantum field theories (IQFT's) has recently received much attention [1–6]. In particular, in reference [1] it was shown that the functional equations for the IQFT “commuting transfer-matrices” introduced in [7] can be transformed [8,9] into integral equations which generalise the standard ground state thermodynamic Bethe Ansatz (TBA) equations to excited states. The results of [1] apply to massive IQFT's obtained from $\phi_{1,3}$ perturbations of the minimal conformal field theory (CFT) models, which are related to the $U_q(\widehat{sl}(2))$ quantum algebra. To include IQFT's related to $\phi_{1,2}$ or $\phi_{2,1}$ perturbations of these minimal CFT models, one has to generalise this approach to the case of the q -deformed twisted Kac-Moody algebra $A_2^{(2)}$. Some results in this direction were obtained in [10,11].

In this paper we consider the IQFT obtained from the perturbation of the non-unitary ($c = -3/5$) minimal CFT $\mathcal{M}_{3,5}$ by its operator $\phi_{2,1}$ with conformal dimensions $\Delta = \bar{\Delta} = 3/4$. It is known that the particle spectrum of this model consists of three kinks of the same mass which interpolate between two degenerate vacuum states. The exact S -matrix of these kinks was conjectured by Smirnov [12]. A numerical study of the energy spectrum of this model was performed in [13] using the Truncated Conformal Space Approach (TCSA) [14]. The TBA equations for the ground state energy were originally conjectured in [15], and more recently, were derived in [16] from the exact S -matrix of the model. In this paper we derive the functional relation for the eigenvalues of the “QFT transfer matrices” which is, in principle, sufficient to determine the whole energy spectrum of the model. In doing this we do not directly follow the route of works [1,7,17], but instead obtain the required functional relation as the scaling limit of the associated lattice model results. Fortunately, a suitable solvable lattice model whose scaling limit describes the above IQFT is known. It is a particular case of the off-critical dilute- A_2 lattice model [18] in a certain regime.

The organisation of the paper is as follows. In Section 2, we briefly review the related results of [16] where the TBA integral equations for the ground state energy of the model were derived using the conventional TBA approach [19,20]. The massive field theory limit of the related dilute- A_2 lattice model is considered in Section 3. In Section 4, we present the functional relation for the QFT transfer matrices along with some numerical results on the positions of zeroes for the largest three eigenvalues of these transfer matrices. Using these results we then derive the TBA-like integral equations which correspond to the ground state and two lowest excited states energies of the finite-size QFT described above. Comparisons are made between the two lowest excited state energy gaps computed from the above TBA-like integral equations and corresponding results [13] of the truncated conformal space approach (TCSA).

2 The S -Matrix and Ground state TBA Equation

Consider the massive QFT described by the action

$$\mathcal{A} = \mathcal{A}_{\mathcal{M}_{3,5}} + g \int \phi_{2,1} d^2x \quad (2.1)$$

where $\mathcal{A}_{\mathcal{M}_{3,5}}$ represents the action of the $c = -3/5$ minimal non-unitary CFT $\mathcal{M}_{3,5}$, the operator $\phi_{2,1}$ has conformal dimensions $(3/4, 3/4)$, and g is a coupling constant of dimension $(\text{mass})^{1/2}$. It is known [21], that this action defines an integrable QFT in the sense that it possesses an infinite number of non-trivial integrals of motion. The particle spectrum of the model consists of three kinks (of the same mass m) interpolating between two degenerate vacuum states (labelled 0 and 1). The precise relationship between the perturbation parameter g and the kink mass m is [22]

$$g = \frac{i \Gamma\left(\frac{5}{12}\right) \Gamma\left(\frac{1}{3}\right)}{2\sqrt{3}\pi \Gamma\left(\frac{7}{12}\right) \Gamma\left(\frac{2}{3}\right)} m^{\frac{1}{2}} \approx 0.25300091957 \dots i m^{\frac{1}{2}}. \quad (2.2)$$

The exact kink-kink S -matrix (as first conjectured in [12]) can be written in the form [13]

$$S_{\alpha\beta}^{\gamma\delta}(\theta) = \left(\frac{\rho_\gamma \rho_\delta}{\rho_\alpha \rho_\beta} \right)^{-\frac{\theta}{2\pi i}} R(\theta) W \left(\begin{array}{cc|c} \alpha & \delta & \varkappa\theta \\ \gamma & \beta & \end{array} \right), \quad \alpha, \beta, \gamma, \delta \in \{0, 1\} \quad (2.3)$$

where θ is the physical rapidity variable, the parameters $\varkappa = -\frac{3i}{5}$, $\rho_0 = 2 \cos \mu$ and $\rho_1 = 1$, and the normalisation factor is

$$R(\theta) = \frac{\sin\left(\frac{2\pi}{5} - \frac{3i\theta}{5}\right) \sin\left(\frac{\pi}{5} - \frac{3i\theta}{5}\right)}{\sin\left(\frac{2\pi}{5} + \frac{3i\theta}{5}\right) \sin\left(\frac{\pi}{5} + \frac{3i\theta}{5}\right)}. \quad (2.4)$$

Here, the functions $W(\dots)$ denote the Boltzmann weights of the critical hard hexagon lattice model [23] (in an unphysical regime). With a suitable normalisation these Boltzmann weights can be expressed as

$$\begin{aligned} W \left(\begin{array}{cc|c} 0 & 0 & u \\ 0 & 0 & \end{array} \right) &= \frac{\sin \mu \sin(2\mu+u)}{\sin 2\mu \sin(\mu-u)} \\ W \left(\begin{array}{cc|c} 0 & 0 & u \\ 1 & 0 & \end{array} \right) &= W \left(\begin{array}{cc|c} 0 & 1 & u \\ 0 & 0 & \end{array} \right) = \left[\frac{\sin \mu}{\sin 2\mu} \right]^{\frac{1}{2}} \frac{\sin u}{\sin(\mu-u)} \\ W \left(\begin{array}{cc|c} 1 & 0 & u \\ 0 & 0 & \end{array} \right) &= W \left(\begin{array}{cc|c} 0 & 0 & u \\ 0 & 1 & \end{array} \right) = 1 \\ W \left(\begin{array}{cc|c} 0 & 1 & u \\ 1 & 0 & \end{array} \right) &= \frac{\sin \mu \sin(2\mu-u)}{\sin 2\mu \sin(\mu-u)} \\ W \left(\begin{array}{cc|c} 1 & 0 & u \\ 0 & 1 & \end{array} \right) &= \frac{\sin(\mu+u)}{\sin(\mu-u)} \end{aligned} \quad (2.5)$$

where $u = \varkappa\theta$ is the lattice spectral parameter and $\mu = 3\pi/5$ is the crossing parameter.

The S -matrix (2.3) defines a factorized scattering theory. This implies that a system of N kinks distributed along a large spatial circle of length L can be analysed via the usual Bethe Ansatz (BA) approach. The rapidities $\theta_1, \dots, \theta_N$ of the respective kinks are consequently constrained by the Bethe-Yang equations [20]

$$e^{imL \sinh \theta_k} \Lambda(\theta_k; \theta_1, \dots, \theta_N) = -1, \quad k = 1, \dots, N \quad (2.6)$$

where $\Lambda(\theta; \theta_1, \dots, \theta_N)$ are the eigenvalues of the ‘‘scattering transfer matrix’’

$$\mathbf{T}(\theta; \theta_1, \dots, \theta_N)_{\{\alpha\}}^{\{\beta\}} = \prod_{i=1}^N S_{\beta_i \alpha_{i+1}}^{\alpha_i \beta_{i+1}}(\theta - \theta_i). \quad (2.7)$$

From equation (2.3) it is obvious that this is just the transfer matrix of the inhomogeneous lattice model with the Boltzmann weights given by (2.5). The eigenvalues of this lattice model were found in [24] using the analytic Bethe Ansatz approach. This result (together with some assumptions on the string structure of the associated Bethe-Ansatz equations) enables one to follow the standard TBA procedure [16]. Below we briefly review these calculations.

The states of the system in the thermodynamic limit $N \rightarrow \infty$, $L \rightarrow \infty$, are specified by the densities of the rapidity distributions for the kinks and quasi-particles arising in the diagonalization of the transfer matrix (2.7). As shown in [16], only one type of quasi-particle is required in our case. The densities of the rapidity distributions for the kink and the quasi-particle (and the associated densities of ‘‘holes’’ in these distributions) are then determined by the following integral equations [16]

$$\frac{m}{2\pi} \delta_{j,0} \cosh \theta = \sigma_j(\theta) + \tilde{\sigma}_j(\theta) + \sum_{k=0}^1 \int_{-\infty}^{\infty} \Phi_{j,k}(\theta - \theta') \sigma_k(\theta') d\theta', \quad j = 0, 1. \quad (2.8)$$

where

$$\Phi_{j,k}(\theta) = (\delta_{j,k} - \delta_{j,k-1} - \delta_{j,k+1}) \phi(\theta), \quad \phi(\theta) = \frac{\sqrt{3} \sinh(2\theta)}{\pi \sinh(3\theta)}. \quad (2.9)$$

Here $\sigma_0(\theta)$ denotes the density of the kink rapidity distribution which is normalised as

$$L \int_{-\infty}^{\infty} \sigma_0(\theta) d\theta = N, \quad (2.10)$$

and $\tilde{\sigma}_0(\theta)$ denotes the corresponding density of ‘‘holes’’ in this distribution. Similarly, $\sigma_1(\theta)$ and $\tilde{\sigma}_1(\theta)$ denote the rapidity and hole densities for the quasi-particles. The density of states in the system is determined by the usual combinatorial entropy [25]

$$\mathcal{S}[\sigma_0(\theta), \sigma_1(\theta)] = L \sum_{k=0}^1 \int_{-\infty}^{\infty} \left\{ [\sigma_j(\theta) + \tilde{\sigma}_j(\theta)] \ln [\sigma_j(\theta) + \tilde{\sigma}_j(\theta)] - \sigma_j(\theta) \ln \sigma_j(\theta) - \tilde{\sigma}_j(\theta) \ln \tilde{\sigma}_j(\theta) \right\} d\theta. \quad (2.11)$$

The free energy of the system is then defined as the functional

$$\mathcal{F}[\sigma_0(\theta), \sigma_1(\theta)] = \mathcal{E}[\sigma_0(\theta)] - \frac{1}{R} \mathcal{S}[\sigma_0(\theta), \sigma_1(\theta)], \quad (2.12)$$

where $1/R$ acts as the temperature parameter, and the energy is

$$\mathcal{E}[\sigma_0(\theta)] = \epsilon L + mL \int_{-\infty}^{\infty} \cosh \theta \sigma_0(\theta) d\theta. \quad (2.13)$$

Here, the parameter

$$\epsilon = m^2 \log(mR_0)/(8\pi) \quad (2.14)$$

is the vacuum energy (per unit length) for the QFT defined by the action (2.1) [15, 22], and R_0 is a non-universal ultraviolet cutoff parameter. Using the standard calculations, one obtains the equilibrium free energy in the form

$$f_0(mR) = \frac{\mathcal{F}}{L} = \epsilon - \frac{m}{2\pi R} \int_{-\infty}^{\infty} \cosh \theta \log \left(1 + e^{-\epsilon_0(\theta)} \right) d\theta \quad (2.15)$$

where the pseudo-energies

$$\varepsilon_j(\theta) = \log \left(\tilde{\sigma}_j(\theta) / \sigma_j(\theta) \right)$$

are determined by the TBA integral equations [15, 16]

$$\varepsilon_j(\theta) = \delta_{j,0} mR \cosh(\theta) + \sum_{k=0}^1 \int_{-\infty}^{\infty} \Phi_{j,k}(\theta - \theta') \log \left(1 + e^{-\varepsilon_k(\theta')} \right) d\theta', \quad j = 0, 1. \quad (2.16)$$

As is well known, the free energy (2.15) can be re-interpreted as the ground state energy

$$E_0(R) = Rf_0(mR) = \frac{m^2 R \log(mR_0)}{8\pi} - \frac{m}{2\pi} \int_{-\infty}^{\infty} \cosh \theta \log \left(1 + e^{-\varepsilon_0(\theta)} \right) d\theta \quad (2.17)$$

of a finite-size system defined on a circle of circumference R . The leading asymptotics of $E_0(R)$ in the ultraviolet limit $R \rightarrow 0$, can be calculated using the standard “dilogarithm trick” [26]. This results in

$$E_0(R) \sim -\frac{\pi}{10R} \quad (2.18)$$

which is in agreement with the expected form $E_0(R) \sim -(\pi/6R)(c-24\Delta_0)$, where $\Delta_0 = -1/20$ is the lowest conformal dimension of the operator algebra associated with the minimal CFT model $\mathcal{M}_{3,5}$.

3 The dilute- A_2 lattice model

The IQFT model considered above is associated with a certain regime of the solvable dilute- A_2 lattice model [18,27]. The general dilute- A_M model is an interaction-round-a-face (IRF) model defined on the square lattice which has discrete spin variables a_i (or “heights”) located at the lattice sites. These heights can take one of M (with $M \geq 2$) possible integer values $1 \leq a_i \leq M$, subject to the restriction that neighbouring sites either have the same height or differ by ± 1 . The explicit expressions for the Boltzmann weights of an elementary face of the lattice are given in Appendix A. They are parameterised through the elliptic theta functions $\vartheta_j(u; p)$ of (spectral) variable u and nome $p = e^{-\tau}$ which are also given in Appendix A. Moreover, these Boltzmann weights depend on an additional parameter λ which should be chosen from the discrete set of values

$$\lambda = \frac{k\pi}{4(M+1)}, \quad k \in \{1, \dots, M, M+2, \dots, 2M+1\}. \quad (3.1)$$

It is only when $k = M$ or $k = M+2$ that the model is physical in the sense that all of the Boltzmann weights are real and positive (for some range of the variable u on the real axis). Here we consider a specific unphysical case (corresponding to $k = 1$ in (3.1)) with

$$M = 2, \quad p > 0, \quad 0 < u < 3\lambda, \quad \lambda = \pi/12. \quad (3.2)$$

We show below that the scaling limit of this model is described by the IQFT considered in the previous sections (*i.e.* the IQFT obtained as a perturbation of the minimal non-unitary CFT $\mathcal{M}_{3,5}$ by its operator $\phi_{2,1}$).

The row-to-row transfer matrix (with periodic boundary conditions in the horizontal direction) is defined by

$$\mathbf{T}_{\{a\}}^{\{b\}}(u) = \prod_{j=1}^N W \left(\begin{array}{c|c} b_j & b_{j+1} \\ a_j & a_{j+1} \end{array} \middle| u \right) \quad (3.3)$$

where $\{a\} = \{a_1, a_2, \dots, a_N\}$ and $\{b\} = \{b_1, b_2, \dots, b_N\}$ denote heights on two consecutive rows of the lattice, periodic boundary conditions imply that $a_{N+1} = a_1$ and $b_{N+1} = b_1$, and N is the number of sites per row. Since the Boltzmann weights of the model satisfy the Yang-Baxter equation [18], the transfer matrices $\mathbf{T}(u)$ with different values of the spectral parameter u commute among themselves (for fixed values of p and λ)

$$[\mathbf{T}(u), \mathbf{T}(u')] = 0 \quad (3.4)$$

and hence can be simultaneously diagonalized. The corresponding eigenvalues of the transfer matrix (3.3) are given by [28]

$$\Lambda(u) = \omega \left(h(2\lambda-u) h(3\lambda-u) \right)^N \frac{Q(u+\lambda)}{Q(u-\lambda)}$$

$$\begin{aligned}
& + \left(h(u) h(3\lambda - u) \right)^N \frac{Q(u) Q(u-3\lambda)}{Q(u-\lambda) Q(u-2\lambda)}, \\
& + \omega^{-1} \left(-h(u) h(\lambda - u) \right)^N \frac{Q(u-4\lambda)}{Q(u-2\lambda)}
\end{aligned} \tag{3.5}$$

where

$$Q(u) = \prod_{j=1}^N h(u - iv_j) \tag{3.6}$$

and where the function $h(u)$ coincides (up to a simple factor) with the standard theta function defined in (A.1)

$$h(u) = p^{-1/4} \vartheta_1(u; p), \quad p = e^{-\tau}. \tag{3.7}$$

The numbers $\{v_j\}$ are solutions of the following set of Bethe Ansatz (BA) equations

$$\omega^{-1} \left(\frac{h(\lambda + iv_j)}{h(\lambda - iv_j)} \right)^N = - \prod_{k=1}^N \frac{h(iv_j - iv_k + 2\lambda) h(iv_j - iv_k - \lambda)}{h(iv_j - iv_k - 2\lambda) h(iv_j - iv_k + \lambda)}, \quad j = 1, \dots, N \tag{3.8}$$

with $\omega = \exp(i\pi m/(M+1))$, $m = 1, \dots, M$.

Now consider the Hamiltonian of the associated one-dimensional quantum spin chain

$$\mathbf{H}_N = -\frac{1}{4\delta} \frac{d}{du} \log \mathbf{T}_N(u) \Big|_{u=0} + \text{const}, \tag{3.9}$$

where δ is a parameter with the dimension of length. The corresponding energy eigenvalues (with a suitable choice of the constant term in (3.9)) can be expressed as

$$E_N = -\frac{1}{4\delta} \frac{d}{du} \sum_{j=1}^N \log \left(\omega \frac{h(u + \lambda - iv_j)}{h(u - \lambda - iv_j)} \right) \Big|_{u=0}. \tag{3.10}$$

The scaling limit of this lattice model can also be analysed within the TBA approach. When $N \rightarrow \infty$ the solutions $\{v_j\}$ of (3.8) converge to certain asymptotic patterns in the complex v -plane, which can be viewed as collections of “strings” [29]. An ℓ -string is a set of $\ell \geq 1$ complex roots with the same real part, symmetric with respect to the real axis of v and equally spaced (with the spacing 2λ) along the imaginary axis. The total number of roots ℓ in a string is called the length of the string. Numerical calculations suggest that for $N \rightarrow \infty$ the string spectrum of (3.8) is saturated by the strings of lengths $\ell = 1, 2, 3$ only (in the sense that the number of strings of other types in a generic solution of (3.8) grows slower than N). Assuming this picture is correct, it is possible to write the roots v_j which solve (3.8) in the form

$$v_{j,k}^{(\ell)} = \frac{1}{4} \theta_j^{(\ell)} + i\Delta_k^{(\ell)} + O(e^{-aN}), \quad k = 1, \dots, \ell, \quad j = 1, \dots, N^{(\ell)}, \quad \ell = 1, 2, 3 \tag{3.11}$$

where

$$\Delta_k^{(\ell)} = \lambda(2k - \ell - 1), \quad (3.12)$$

and the (real) numbers $\theta_j^{(\ell)}$ determine the centres of the strings. It is to be noted that for non-vanishing values of the elliptic nome $p > 0$ the convergence parameter a in (3.11) is positive and non-zero. The integers $N^{(\ell)}$ denote the total number of strings of length ℓ in a particular solution of (3.8). As follows from (3.6) these numbers are restricted by

$$\sum_{\ell=1}^3 \ell N^{(\ell)} = N + o(N). \quad (3.13)$$

In the thermodynamic limit $N \rightarrow \infty$, the centres of the strings form continuous distributions and the BA equations (3.8) lead to the following integral equations¹ for the densities of strings $\rho_\ell(\theta)$ and ‘‘holes’’ $\tilde{\rho}_\ell(\theta)$ [19]

$$b_s(\theta) = \tilde{\rho}_s(\theta) + \rho_s(\theta) + \sum_{t=1}^3 \int_{-2\tau}^{2\tau} B_{s,t}(\theta - \theta') \rho_t(\theta') d\theta', \quad s, t = 1, \dots, 3, \quad (3.14)$$

where

$$b_s(\theta) = \sum_{k=1}^s a_2 \left(\theta + i\Delta_k^{(s)} \right) \quad (3.15)$$

$$B_{s,t}(\theta) = \sum_{k=1}^s \sum_{m=1}^t \left[a_4 \left(\theta + i\Delta_k^{(s)} + i\Delta_m^{(t)} \right) - a_2 \left(\theta + i\Delta_k^{(s)} + i\Delta_m^{(t)} \right) \right] \quad (3.16)$$

and where the function $a_j(\theta)$ is defined as

$$a_j(\theta) = \frac{1}{2\pi i} \frac{d}{d\theta} \log \left[\frac{h(\lambda j/2 + i\theta/4)}{h(\lambda j/2 - i\theta/4)} \right]. \quad (3.17)$$

Note that the functions $a_j(\theta)$ (as well as $b_s(\theta)$, $B_{s,t}(\theta)$ and all of the densities $\rho_\ell(\theta)$ and $\tilde{\rho}_\ell(\theta)$) are periodic with period 4τ . Also, the densities ρ_ℓ are normalised by the condition

$$\int_{-2\tau}^{2\tau} \rho_\ell(\theta) d\theta = N^{(\ell)}/N \quad (3.18)$$

which from (3.13) implies that

$$\sum_{\ell=1}^3 \int_{-2\tau}^{2\tau} \ell \rho_s(\theta) d\theta = 1. \quad (3.19)$$

¹ This approximation is valid provided $Np^2 \gg 1$ in addition to $N \gg 1$. In this section we will assume that this extra condition is also satisfied.

This relation together with equation (3.14) (with $s = 3$) implies that $\tilde{\rho}_3(\theta) \equiv 0$, and hence it is possible to eliminate the density $\rho_3(\theta)$ from (3.14). Re-denoting the remaining densities as

$$\begin{aligned}\rho_1(\theta) &\equiv \delta \tilde{\sigma}_0(\theta+2\tau), & \tilde{\rho}_1(\theta) &\equiv \delta \sigma_0(\theta+2\tau) \\ \rho_2(\theta) &\equiv \delta \sigma_1(\theta+2\tau), & \tilde{\rho}_2(\theta) &\equiv \delta \tilde{\sigma}_1(\theta+2\tau)\end{aligned}\quad (3.20)$$

where the parameter δ is the same as in (3.9), one obtains the integral equations

$$\delta^{-1} \delta_{j,0} \phi_0(\theta+2\tau, \tau) = \sigma_j(\theta) + \tilde{\sigma}_j(\theta) + \sum_{k=0}^1 \int_{-\infty}^{\infty} \Phi_{j,k}(\theta-\theta', \tau) \sigma_k(\theta') d\theta', \quad j = 0, 1. \quad (3.21)$$

Here, the functions

$$\Phi_{j,k}(\theta, \tau) = (\delta_{j,k} - \delta_{j,k-1} - \delta_{j,k+1}) \phi_0(\theta, \tau) \quad (3.22)$$

$$\phi_0(\theta, \tau) = \frac{1}{4\tau} \sum_{n=-\infty}^{\infty} e^{i\theta x_n} \frac{\cosh(2\lambda x_n)}{\cosh(6\lambda x_n)}, \quad x_n = \frac{\pi n}{2\tau}, \quad (3.23)$$

and the parameter $\lambda = \pi/12$. The largest eigenvalue $\Lambda_0(u)$ of the transfer matrix (3.3) (and hence the ground state energy of the Hamiltonian (3.9)) is determined by the solution of (3.8) that consists only of 1-strings. The corresponding density

$$\rho_1^{(vac)}(\theta) = \phi_0(\theta, \tau) \quad (3.24)$$

can be easily determined from (3.21). Then from (3.5) one obtains

$$\log \kappa(u) = \lim_{N \rightarrow \infty} \left(\frac{1}{N} \log \Lambda_0(u) \right) = \log \rho + \int_{-2\tau}^{2\tau} \log \left(\frac{\vartheta_1(u+\lambda+i\theta/4) \vartheta_1(4\lambda-u+i\theta/4)}{\vartheta_1(\lambda+i\theta/4) \vartheta_1(4\lambda+i\theta/4)} \right) \phi_0(\theta, \tau) d\theta \quad (3.25)$$

where

$$\rho = h(2\lambda)h(3\lambda). \quad (3.26)$$

Finally, the spectrum of the Hamiltonian (3.10) for large N reads

$$E_N = -\frac{N}{4\delta} \frac{d}{du} \log \kappa(u) \Big|_{u=0} + 2\pi N \int_{-2\tau}^{2\tau} \phi_0(\theta+2\tau, \tau) \sigma_0(\theta) d\theta \quad (3.27)$$

where the first term represents the vacuum energy and the second term represents the excitation energy. The gap in the excitation spectrum is then determined by the value of $\phi_0(\theta+2\tau, \tau)$ at $\theta = 0$ where the one-particle excitation energy has a minimum.

Now consider the scaling limit. The leading singularity of (3.25) for $p \rightarrow 0$ is given by

$$\log \kappa(u)_{\text{sing}} = -\frac{12 \sin 4u}{\pi} p^4 \log p \quad (3.28)$$

which determines the thermal exponent α and correlation length exponent ν to be

$$2 - \alpha = 4, \quad \nu = 2. \quad (3.29)$$

Let us now identify the parameter δ in (3.9) with the lattice spacing constant, and take the limits $N \rightarrow \infty$ and $\delta \rightarrow 0$, while keeping both the (dimensional) length of the chain $L = N\delta$ and the correlation length $R_c \sim p^{-\nu}\delta$ finite. This means that

$$p^2 \sim N^{-1}, \quad \delta \sim N^{-1}, \quad N \rightarrow \infty. \quad (3.30)$$

We shall also assume that $L \gg R_c$ (which is equivalent to $Np^2 \gg 1$, see footnote 1 on page 8). In the above limit, the gap m in the one-particle spectrum of (3.27) (*i.e.* the mass gap) tends to a finite value. Indeed, one has

$$2\pi\delta^{-1}\phi_0(\theta+2\tau, \tau) = m \cosh \theta + O(p^2), \quad p \rightarrow 0, \quad (3.31)$$

where

$$m = 4\sqrt{3}p^2\delta^{-1}, \quad (3.32)$$

and hence expression (3.27) becomes

$$E(L) = \frac{m^2 L \log(mL_0)}{8\pi} + mL \int_{-\infty}^{\infty} \cosh \theta \sigma_0 d\theta. \quad (3.33)$$

It is to be noted that the bulk vacuum energy term here is determined entirely by the singular part (3.28) of the largest eigenvalue of the transfer matrix. The parameter L_0 is non-universal, and in particular, it depends on an overall shift of the energy spectrum in (3.9). It is obvious that the energy expression (3.33) is identical to that given by (2.13) and (2.14) of the previous section. Similarly, using (3.31) and

$$\phi_0(\theta, \tau) = \phi(\theta) + O(p^2), \quad p \rightarrow 0 \quad (3.34)$$

with $\phi(\theta)$ given by (2.9), it is easy to see that the integral equations (3.21) in the limit (3.30) become identical to (2.8). And finally, the density of states in this lattice model is, of course, determined by exactly the same combinatorial entropy functional as in (2.11).

4 Excited states energies for the finite-size system

In the previous section we established an equivalence between the QFT (2.1) and the scaling limit of the dilute A_2 lattice model. We have shown that the density of states in these two systems are described by the same integral equations. This means, in particular, that they also

have the same finite-volume ground state energy (as determined by the TBA approach). It is natural to expect that this correspondence extends to all (finite-volume) excitation energies.

An effective way to extract information about the spectrum of the transfer matrix in lattice models is to use the functional relations. Using the standard fusion procedure, it is not difficult to show by explicit calculations² that in the case of the dilute- A_2 model considered here, the transfer matrix (3.3) (and hence all of its eigenvalues) satisfies the relation

$$\mathbf{T}(u+\pi/12)\mathbf{T}(u-\pi/12) = a(u)\mathbf{T}(u+\pi/2) + (-1)^N b(u)\mathbf{T}(u) \quad (4.1)$$

where N is the number of sites per row (which hereafter is assumed to be even), and the scalar coefficients read

$$a(u) = (h(u - \pi/12)h(u - \pi/6))^N, \quad b(u) = (h(u + \pi/12)h(u - \pi/3))^N. \quad (4.2)$$

In references [8,9], Klümper and Pearce developed a technique for transforming functional relations of the form (4.1) to integral equations. This is particularly useful in studying the eigenvalues of the transfer matrix for finite values of N . To apply this technique one first requires information on the patterns of zeroes of the eigenvalues. We have used numerical calculations to study these patterns as follows.

For small system sizes all solutions to the Bethe-Ansatz equations (3.8) are easily found numerically using standard nonlinear equation solving algorithms. The eigenvalue expressions (3.5) corresponding to these BA solutions, can then be compared against the results of the direct numerical diagonalization of the transfer matrix (3.3). This enables one to numerically determine the patterns of zeroes of $\Lambda(u)$ (or equivalently, patterns of zeroes of $Q(u)$) corresponding to each eigenvalue of the transfer matrix (3.3). The results obtained for the largest and a few next-to-largest eigenvalues of the transfer matrix $\mathbf{T}(u)$ are presented below. In the following, it will be convenient to use a new spectral variable θ , which is related to the variable u by

$$\theta = -4i(u - \pi/8 - i\tau/2). \quad (4.3)$$

To make this change more explicit we denote the eigenvalues of the transfer matrix as $T(\theta) \equiv \Lambda(u)$ (assuming that θ and u are always related by (4.3)). The eigenvalues $T(\theta)$ are entire functions of θ satisfying the (quasi-) periodicity relations

$$T(\theta+4\pi i) = T(\theta), \quad T(\theta+4\tau) = \exp[N(\theta+4\tau)]T(\theta). \quad (4.4)$$

In fact, these eigenvalues can be written as the products

$$T(\theta) = C e^{\alpha\theta} \prod_{j=1}^{2N} \vartheta_1\left(i(\theta-\theta_j)/4\right) \quad (4.5)$$

²See also Sect.5.3 below.

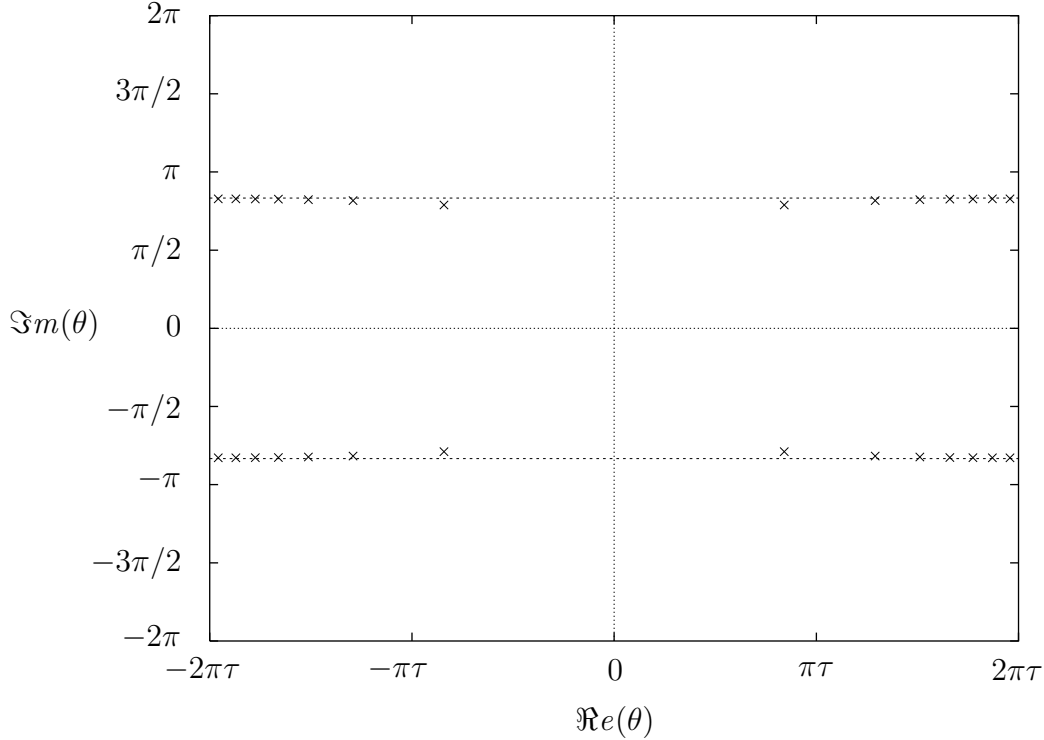


Figure 1: Zeroes of the largest eigenvalue $T_0(\theta)$ for $N = 14$ and $p = 0.1$.

where C and $\alpha = \sum_{j=1}^{2N} \theta_j$ are some constants and θ_j denote the zeroes of $T(\theta)$. The patterns of these zeroes for the three largest eigenvalues (which we denote as $T^{(0)}(\theta)$, $T^{(1)}(\theta)$ and $T^{(2)}(\theta)$) with $p = 0.1$, obtained numerically for $N = 14$ sites per row are shown in Figures 1, 2 and 3a respectively. The zeroes of $T^{(2)}(\theta)$ with $p = 0.3$ are also shown in Figure 3b to emphasise the qualitative change in the position of two of the zeroes at some intermediate value of p . The total number of zeroes in each of the figures is equal to $2N = 28$. As can be seen from the figures, most of the zeroes accumulate near the lines

$$\Im m \theta = \pm \frac{5\pi}{6}. \quad (4.6)$$

In fact, for the largest eigenvalue $T^{(0)}(\theta)$ all of the zeroes are located near these lines. The eigenvalue of the first excited state $T^{(1)}(\theta)$ has two zeroes shifted to the positions

$$\theta = \pm i\pi + O(p). \quad (4.7)$$

The eigenvalue of the second excited state $T_2(\theta)$ also has two shifted zeroes similar to (4.7), and in addition, has two more shifted zeroes inside the strip $|\Im m \theta| < \pi/6$ which are located at

$$\theta = \pm \gamma. \quad (4.8)$$

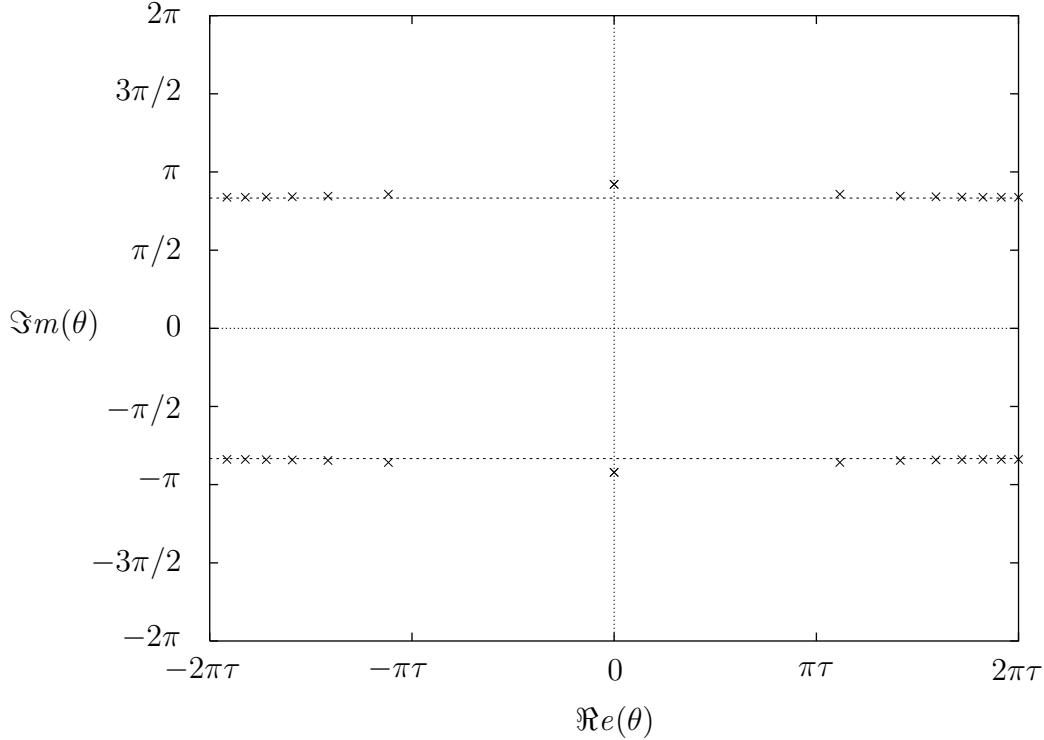


Figure 2: Zeroes of the 2nd largest eigenvalue $T_1(\theta)$ for $N = 14$ and $p = 0.1$.

The value of γ is controlled by the dimensionless scaling parameter

$$r = 4\sqrt{3}p^2 N. \quad (4.9)$$

Numerical calculations show that γ vanishes when r approaches some critical value³ r_c

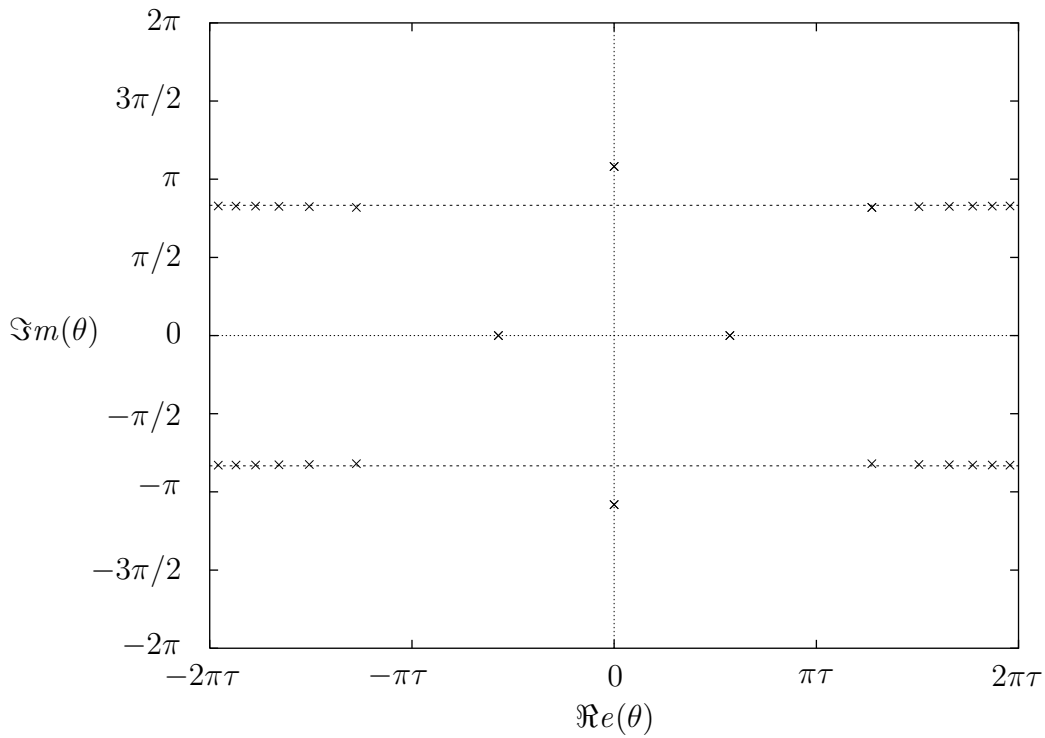
$$\gamma = 0, \quad \text{for} \quad r = r_c \approx 2.85 \pm 0.10 \quad (4.10)$$

For $r > r_c$ the parameter γ is purely imaginary and approaches the value $\gamma_\infty = i\pi/6$ as $r \rightarrow \infty$. For $r < r_c$ the parameter γ is real and increases as $O(|\log r|)$ when $r \rightarrow 0$. We found also that the ratio $T(\theta)/T(\theta+2\pi i)$ satisfies the condition

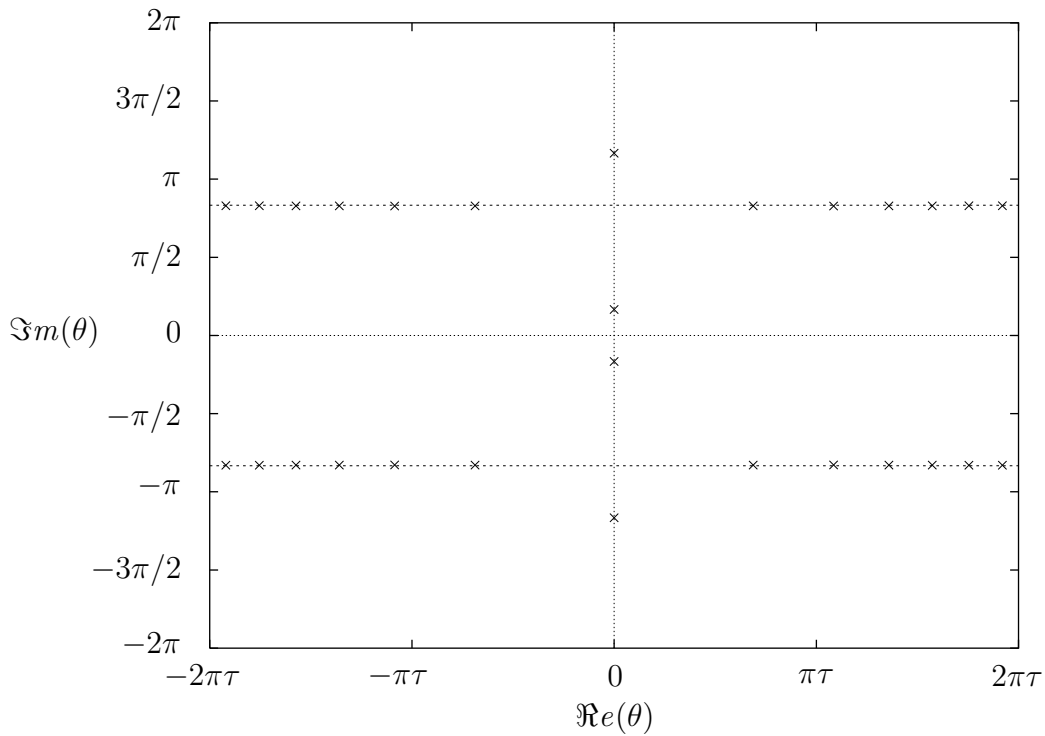
$$T(\theta)/T(\theta+2\pi i) \in \mathbb{R}, \quad \text{for} \quad \Im m(\theta) = 0. \quad (4.11)$$

In fact, this ratio is positive for $T^{(0)}(\theta)$, and for $T^{(2)}(\theta)$ when $r > r_c$, and is negative for $T^{(1)}(\theta)$. For $T^{(2)}(\theta)$ with $r < r_c$, it is negative between the zeroes in (4.8) (*i.e.* for $|\theta| < \gamma$). Here, we assume that these properties of $T^{(0)}(\theta)$, $T^{(1)}(\theta)$ and $T^{(2)}(\theta)$ remain applicable for all arbitrarily large values of N , and small p .

³Note, that an accurate value of this critical value r_c is quite difficult to obtain due to the singular nature of this point which leads to severe numerical instabilities.



(a)



(b)

Figure 3: (a) Zeroes of the 3rd largest eigenvalue $T_2(\theta)$ for $N = 14$ and $p = 0.1$, which corresponds to $r < r_c$; (b) Zeroes of the 3rd largest eigenvalue $T_2(\theta)$ for $N = 14$ and $p = 0.3$, which corresponds to $r > r_c$.

For the following calculations it is convenient to pass directly to the scaling limit (3.30), defining the mass parameter m and the system size R as

$$m = 4\sqrt{3}p^2\delta^{-1}, \quad R = N\delta \quad (4.12)$$

where δ is the dimensional lattice spacing parameter. In this limit, the appropriately normalised eigenvalues of the transfer matrix tend to the finite values

$$\mathbb{T}(\theta) = e^{\frac{r}{2\sqrt{3}}} \lim_{N \rightarrow \infty} \left[\exp \left(c_1 N^{\frac{1}{2}} \cosh(\theta/2) + c_2 \log N \cosh \theta \right) T(\theta) \right] \quad (4.13)$$

where the exponential multiplier in front of the limit sign is introduced for later convenience. The constants c_1 and c_2 should be chosen to regularize the product over zeroes in (4.5) which diverges in this limit. Estimating the asymptotic density of zeros θ_j for large θ from the Bethe Ansatz equations (3.8), one can show that

$$c_1 = \frac{r^{\frac{1}{2}}}{3^{\frac{1}{4}}\sqrt{2}} \quad (4.14)$$

where $r = mR$ is the dimensionless scaling parameter previously defined in (4.9). Although it is also possible to calculate the value of the constant c_2 , this is not essential for the following discussion and is hence omitted here. It can be shown from the properties (4.4), that the functions $\mathbb{T}(\theta)$ defined in (4.13), are entire functions of the variable θ which obey the periodicity relation

$$\mathbb{T}(\theta+4\pi i) = \mathbb{T}(\theta) \quad (4.15)$$

and have the following asymptotic behaviour for $\theta \rightarrow \pm\infty$

$$\begin{aligned} \log \left| \mathbb{T}(\theta) \right| &\sim \mp \frac{\sqrt{3}r}{8\pi} \theta e^{\pm\theta} + c_3 e^{\pm\theta} + O(e^{\mp\theta}) \\ \log \left| \mathbb{T}(\theta)/\mathbb{T}(\theta+2\pi i) \right| &\sim \frac{r}{2} e^{\pm\theta} + O(e^{\mp\theta}) \end{aligned} \quad (4.16)$$

where c_3 is some (unknown) constant. These asymptotics are valid in the strip⁴ $|\Im m \theta| < \pi/3$. The functions $\mathbb{T}(\theta)$ are in fact the QFT counterparts of the eigenvalues of the transfer matrix of the lattice model. Using (4.1) and (4.13) it is easy to see that they satisfy the functional relation

$$\mathbb{T}(\theta+i\pi/3)\mathbb{T}(\theta-i\pi/3) = e^{\frac{r}{4} \cosh \theta} \mathbb{T}(\theta) + e^{-\frac{r}{4} \cosh \theta} \mathbb{T}(\theta + 2\pi i). \quad (4.17)$$

Introducing the new functions

$$\mathbb{Y}_0(\theta) = e^{\frac{1}{2}r \cosh \theta} \mathbb{T}(\theta)/\mathbb{T}(\theta+2\pi i), \quad \mathbb{Y}_1(\theta) = \mathbb{Y}_0(\theta+2\pi i) \quad (4.18)$$

⁴In fact, these asymptotics are valid in a wider strip $|\Im m \theta| < 5\pi/6 - \epsilon$ for arbitrary small positive ϵ .

one can then rewrite the functional relation (4.17) in the form

$$\frac{\mathbb{Y}_0(\theta+i\pi/3)\mathbb{Y}_0(\theta-i\pi/3)}{\mathbb{Y}_0(\theta)} = \frac{1 + \mathbb{Y}_0^{-1}(\theta)}{1 + \mathbb{Y}_1^{-1}(\theta)}. \quad (4.19)$$

The asymptotic behaviour of the functions $\mathbb{Y}_{0,1}(\theta)$ at $\theta \rightarrow \pm\infty$ is determined by (4.16) to be

$$\log |\mathbb{Y}_0(\theta)| = \frac{r}{2} e^{\pm\theta} + O(e^{\mp\theta}), \quad \log |\mathbb{Y}_1(\theta)| = O(e^{\mp\theta}), \quad |\Im m \theta| < \pi/3. \quad (4.20)$$

The derivation of the Klümper-Pearce equations for the finite-size energies of the QFT (2.1), is based on the following simple fact [1] that if $f(\theta)$ is a function which is regular, bounded in the strip $|\Im m(\theta)| < \pi/3$, and satisfies the relation

$$f(\theta+i\pi/3) + f(\theta-i\pi/3) - f(\theta) = g(\theta) \quad (4.21)$$

for some function $g(\theta)$, then

$$f(\theta) = \int_{-\infty}^{\infty} d\theta' \phi(\theta-\theta') g(\theta'), \quad (4.22)$$

where $\phi(\theta)$ is defined in (2.9).

The eqs.(4.21),(4.22) combined with knowledge of the analytic properties and asymptotic behaviour of the functions $\mathbb{Y}_{0,1}(\theta)$ defined in (4.19), allows one to rewrite the functional equation (4.19) in terms of nonlinear integral equations which generalise the TBA equations. From the functional equation (4.19), it is easy to see that the simplest case where $\mathbb{Y}_0(\theta)$ and $\mathbb{Y}_1(\theta)$ have no zeroes in the strip $\Im m(\theta) \in (-\pi/3, \pi/3)$, only requires a straightforward application of the lemma (see Section 4.1 below for further details). From Figures 1, 2, 3a and 3b, it can be seen that the only complication arising for the next few largest eigenvalues involves the function $\mathbb{T}(\theta)$ having a finite number of zeroes in the strip $|\Im m \theta| < \pi/3$, which are either real or occur in complex conjugated pairs. Suppose now, for generality, that the function $\mathbb{T}(\theta)$ has a total of $A + 2B$ zeroes in this strip where there are A real zeroes α_a , $a = 1, \dots, A$, and B complex conjugated pairs $\beta_b \pm i\gamma_b$, $b = 1, \dots, B$. Then using (4.17) and (4.18) it is easy to show that the eigenvalue expression (3.10) in the scaling limit (3.30) can then be written as

$$E(R) = \frac{m^2 R \log(mR_0)}{8\pi} + \frac{\sqrt{3}m}{2} \sum_{a=1}^A e^{\alpha_a} + 2m \sum_{b=1}^B \cosh \beta_b \sin \left(\frac{\pi}{3} - \gamma_b \right) - \frac{m}{2\pi} \int_{-\infty}^{\infty} \cosh \theta \log \left| 1 + \mathbb{Y}_0(\theta)^{-1} \right| d\theta. \quad (4.23)$$

In Sections 4.1-4.3 below, we explicitly study the form of the resulting TBA integral equations and energies corresponding to the ground state and first two excited state energies of the spectrum (3.10).

4.1 The TBA Equations for the Ground State

As follows from the discussion of the properties of the eigenvalues of the transfer matrix at the beginning of the previous section, and as shown explicitly in Figure 1, all of the zeroes of the functions $\mathbb{T}(\theta)$ and $\mathbb{T}(\theta+2\pi i)$ are in this case located in the vicinity of the lines $\Im m(\theta) = \pm 5\pi/6$ and $\Im m(\theta) = \pm 7\pi/6$ respectively. In particular, they do not contain any zeroes in the strip $|\Im m(\theta)| < \pi/3$. Moreover, their ratio is real and positive for all real θ . Therefore the functions

$$\epsilon_0(\theta) = \log \mathbb{Y}_0(\theta), \quad \epsilon_1(\theta) = \log \mathbb{Y}_1(\theta) \quad (4.24)$$

are real analytic for $|\Im m(\theta)| < \pi/3$. Taking into account the asymptotics (4.20), it follows that the functions $\epsilon_0(\theta) - r \cosh \theta$ and $\epsilon_1(\theta)$ are regular and bounded in the strip $|\Im m(\theta)| < \pi/3$. Therefore one can bring [1] the functional relation (4.19) to the form

$$\epsilon_j(\theta) = \delta_{j,0} mR \cosh \theta + \sum_{k=0}^1 \Phi_{j,k} * L_k^{(-)}(\theta), \quad j = 0, 1 \quad (4.25)$$

where the kernel $\Phi_{j,k}(\theta)$ and the function $L_k^{(\pm)}(\theta)$, are respectively defined by

$$\Phi_{j,k}(\theta) = (\delta_{j,k} - \delta_{j,k-1} - \delta_{j,k+1}) \phi(\theta) \quad (4.26)$$

$$L_k^{(\pm)}(\theta) = \log (1 + e^{\pm \epsilon_k(\theta)}), \quad (4.27)$$

the function $\phi(\theta)$ is defined in (2.9), and the convolution operator $*$ is defined by

$$f * g(\theta) = \int_{-\infty}^{\infty} f(\theta - \theta') g(\theta') d\theta'. \quad (4.28)$$

Equations (4.25) are identical to the TBA integral equations (2.16). Similarly, the energy expression (4.23) becomes

$$E_0(R) = \frac{m^2 R \log(mR_0)}{8\pi} - \frac{m}{2\pi} \int_{-\infty}^{\infty} \cosh \theta L_0^{(-)}(\theta) d\theta. \quad (4.29)$$

which is also identical to the earlier TBA result (2.17), at least up to some appropriate bulk term. Consequently, the conformal properties associated with the scaling limit of these equations are the same as those calculated in section 2.

4.2 The TBA Equations for the First Excited State

As shown in Figure 2, the location of the zeroes of $\mathbb{T}(\theta)$ and $\mathbb{T}(\theta+2\pi i)$, is the same as above except that both of these functions have two extra zeroes (4.8) at $\theta = \pm i\pi$. These extra zeroes

cancel out in (4.18) resulting in the functions $\mathbb{Y}_0(\theta)$ and $\mathbb{Y}_1(\theta)$ being real and negative for all real θ . Defining the functions

$$\epsilon_0(\theta) = \log(-\mathbb{Y}_0(\theta)), \quad \epsilon_1(\theta) = \log(-\mathbb{Y}_1(\theta)), \quad (4.30)$$

and proceeding as in the case of the ground state, one obtains from the functional relation (4.19) and energy expression (4.23), the first excited state TBA equations

$$\epsilon_j(\theta) = \delta_{j,0} mR \cosh(\theta) + \sum_{k=0}^1 \Phi_{j,k} * \log\left(1 - e^{-\epsilon_k(\theta)}\right), \quad j = 0, 1, \quad (4.31)$$

where the function $\Phi_{j,k}(\theta)$ is defined in (4.26), and the corresponding first excited state energy

$$E_1(R) = \frac{m^2 R \log(mR_0)}{8\pi} - \frac{m}{2\pi} \int_{-\infty}^{\infty} \cosh \theta \log\left(1 - e^{-\epsilon_0(\theta)}\right) d\theta. \quad (4.32)$$

The leading short distance asymptotics of $E_1(R)$ determined by these equations can be shown using the standard dilogarithm trick [26] to be

$$E_1(R) \sim \frac{\pi}{10R} \quad (4.33)$$

which is in agreement with the expected form $E_1(R) \sim -(\pi/6R)(c - 24\Delta_1)$, where $\Delta_1 = 0$ is the second lowest conformal dimension in the operator algebra associated with the minimal CFT model $\mathcal{M}_{3,5}$. Equations (4.31) and (4.32) were previously conjectured in [15] using a different approach.

4.3 The TBA Equations for the Second Excited State

The location of the zeroes of $\mathbb{T}(\theta)$ and $\mathbb{T}(\theta+2\pi i)$ in this case depends on the value of the parameter r . As described in the previous section (and shown in Figures 3a and 3b), most of the zeroes of these functions are the same as for the first excited state except that there is an extra pair of zeroes. The positions of these extra zeroes depends upon whether the parameter $r < r_c$ or $r > r_c$, where the critical value r_c is specified in (4.10). For $r < r_c$, the extra zeroes of $\mathbb{T}(\theta)$ lie on the real θ axis at the positions $\theta = \pm\alpha$, $\alpha > 0$. For $r > r_c$, the extra zeroes of $\mathbb{T}(\theta)$ lie on the imaginary θ axis at the positions $\theta = \pm i\gamma$, $\gamma > 0$. These two cases are described separately below.

The case $r < r_c$: As follows from the patterns of zeros described above, the function $\mathbb{Y}_0(\theta)$ has two zeroes in the strip $|\Im m(\theta)| < \pi/3$ located on the real θ axis at $\theta = \pm\alpha$, $\alpha > 0$. Correspondingly, the function $\mathbb{Y}_1(\theta)$ has simple poles at these points. Moreover, the large θ

asymptotics of $\mathbb{Y}_0(\theta)$ and $\mathbb{Y}_1(\theta)$ are given by (4.20). This situation is very similar to that described in Reference [1] for the first excited state of the scaling Lee-Yang model. Following the discussion presented there, it is useful to introduce the functions

$$\begin{aligned}\sigma_0(\theta, \alpha) &= \tanh\left(\frac{3}{4}(\theta - \alpha)\right) \\ \sigma_1(\theta, \eta) &= \frac{\cosh(\theta) - \cos(\eta)}{\cosh(\theta) + \cos(\eta)} \frac{\cosh(\theta) - \sin(\pi/6 - \eta)}{\cosh(\theta) + \sin(\pi/6 - \eta)}\end{aligned}\quad (4.34)$$

which satisfy the equations

$$\sigma_0(\theta + i\pi/3) \sigma_0(\theta - i\pi/3) = 1, \quad \sigma_1(\theta + i\pi/3, \eta) \sigma_1(\theta - i\pi/3, \eta) = \sigma_1(\theta, \eta). \quad (4.35)$$

Now, defining the functions

$$\epsilon_0(\theta) = \log \mathbb{Y}_0(\theta) - \log \sigma(\theta, \alpha), \quad \epsilon_1(\theta) = \log \mathbb{Y}_1(\theta) + \log \sigma(\theta, \alpha), \quad (4.36)$$

where

$$\sigma(\theta, \alpha) = \sigma_0(\theta, \alpha) \sigma_0(\theta, -\alpha), \quad (4.37)$$

it then follows that the functions $\epsilon_0(\theta) - r \cosh \theta$ and $\epsilon_1(\theta)$ are regular and bounded in the strip $|\Im m \theta| < \pi/3$. Applying the above lemma one then obtains from (4.19) the integral equations

$$\begin{aligned}\epsilon_0(\theta) &= r \cosh(\theta) + \int_{-\infty}^{\infty} \phi(\theta - \theta') \left[\log \left(\sigma(\theta, \alpha) + e^{-\epsilon_0(\theta')} \right) - \right. \\ &\quad \left. - \log \left(1 + \sigma(\theta, \alpha) e^{-\epsilon_1(\theta')} \right) \right] d\theta' \\ \epsilon_1(\theta) &= r \cosh \theta - \epsilon_0(\theta)\end{aligned}\quad (4.38)$$

where $\phi(\theta)$ is defined in (2.9). The value of α which determines the position of the zeroes of $\mathbb{Y}_0(\theta)$, is constrained by the functional equation (4.17). Indeed, substituting $\theta = \alpha \pm i\pi/3$ in (4.17) results in the condition

$$\mathbb{Y}_0(\alpha \pm i\pi/3) = -1. \quad (4.39)$$

Using the TBA equations (4.38), and the explicit form (2.9) of the kernel $\phi(\theta)$, one can rewrite this condition as

$$\begin{aligned}r\sqrt{3} \sinh \alpha + \frac{3}{\pi} \int_{-\infty}^{\infty} \frac{\cosh 2(\theta - \alpha)}{\sinh 2(\theta - \alpha)} \left[\log \left(\sigma(\theta, \alpha) + e^{-\epsilon_0(\theta')} \right) - \right. \\ \left. - \log \left(1 + \sigma(\theta, \alpha) e^{-\epsilon_1(\theta')} \right) \right] d\theta' = \pi \left(4I + 2 \arctan(\sinh 3\alpha) \right)\end{aligned}\quad (4.40)$$

where I is some integer (arising when taking the logarithm of (4.38)), and where $\int_{-\infty}^{\infty}$ denotes the principal value of the singular integral. Numerical calculations indicate that in this case

$I = 0$. Finally, the energy expression (4.23) in the case $r < r_c$ becomes

$$\begin{aligned} E_2(R) &= \frac{m^2 R \log(mR_0)}{8\pi} + \sqrt{3}m \cosh \alpha - \frac{m}{2\pi} \int_{-\infty}^{\infty} \cosh \theta \log \left| 1 + \mathbb{Y}_0(\theta)^{-1} \right| d\theta. \\ &= \frac{m^2 R \log(mR_0)}{8\pi} - \frac{m}{2\pi} \int_{-\infty}^{\infty} \cosh \theta \log \left(\sigma(\theta, \alpha) + e^{-\varepsilon_0(\theta)} \right) d\theta, \end{aligned} \quad (4.41)$$

Again, the leading short distance asymptotics of $E_2(R)$ can be found through an appropriate modification of the dilogarithm trick [1, 9, 33]. It is not necessary to present further details of this calculation here as they are well described in Appendix C of Reference [1]. The final result is

$$E_2(R) \sim \frac{9\pi}{10R} \quad (4.42)$$

which is in agreement with the expected form $E_2 \sim -(\pi/6R)(c-24\Delta_2)$, where $\Delta_2 = 1/5$ is the third lowest conformal dimension in the operator algebra associated with the minimal CFT model $\mathcal{M}_{3/5}$.

The case $r > r_c$: The consideration of this case is very similar to the case $r < r_c$ described above. The function $\mathbb{Y}_0(\theta)$ (and respectively $\mathbb{Y}_1(\theta)$) has two complex conjugated zeroes (poles) at $\theta = \pm i\gamma$, $\gamma > 0$. Proceeding in the same manner as presented above, one obtains from (4.19)

$$\begin{aligned} \varepsilon_0(\theta) &= r \cosh(\theta) + \log \sigma_1(\theta, \gamma) + \phi * \left[L_0^{(-)}(\theta) - L_1^{(-)}(\theta) \right] \\ \varepsilon_1(\theta) &= r \cosh \theta - \varepsilon_0(\theta) \end{aligned} \quad (4.43)$$

where

$$\varepsilon_0(\theta) = \log \mathbb{Y}_0(\theta), \quad \varepsilon_1(\theta) = \log \mathbb{Y}_1(\theta). \quad (4.44)$$

The value of γ is here determined by the condition

$$\mathbb{Y}_0(\pm i(\gamma - \pi/3)) = -1. \quad (4.45)$$

The corresponding energy expression for $r > r_c$ is

$$E_2(R) = \frac{m^2 R \log(mR_0)}{8\pi} + 2m \sin(\pi/3 - \gamma) - \frac{m}{2\pi} \int_{-\infty}^{\infty} \cosh \theta \log \left(1 + \mathbb{Y}_0(\theta)^{-1} \right) d\theta. \quad (4.46)$$

5 Numerical Results and Discussion

5.1 Numerical results

In order to numerically determine the ground state and lowest two excited state energy levels $E_0(R)$, $E_1(R)$ and $E_2(R)$ as a function of the finite length R , it is first necessary to numerically

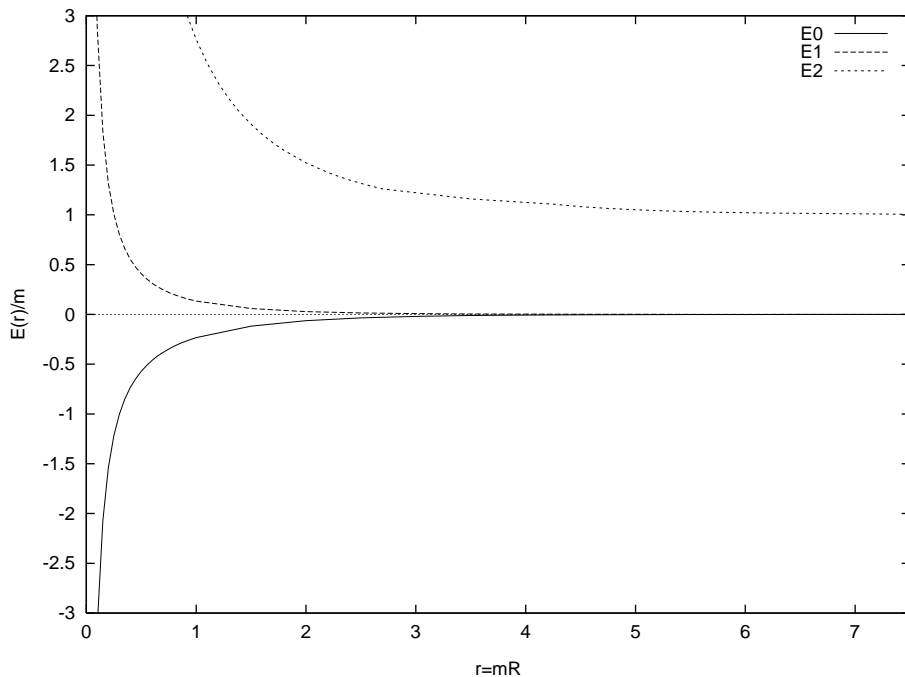


Figure 4: The lowest three energy levels $E_0(R)$, $E_1(R)$ and $E_2(R)$ of the $\mathcal{M}_{3,5} \pm \phi_{2,1}$ QFT obtained numerically from the energy expressions (4.29), (4.32), (4.41) and (4.46), after numerically solving the respective TBA integral equations (4.25), (4.31), (4.38) with the constraint (4.40), and (4.43) with the constraint (4.45).

solve the respective systems of TBA integral equations for all required values of R . In the case of the ground state energy $E_0(R)$, the associated TBA equations (4.25) are easily solved at particular values⁵ of R using a simple iterative procedure. Using these solutions it is then straightforward to numerically integrate the energy expression (4.29) to obtain $E_0(R)$ at these values of R .

For the first excited state energy level $E_1(R)$ defined by (4.32), the associated TBA equations (4.31) can again be solved numerically at particular values of R using a simple iterative procedure. The only significant difference in this case, is that there are convergence problems which can arise due to the fact that it is now possible for the argument of the logarithmic term in (4.31) to become either very small, or even negative. Once a numerical solution of (4.31) is known, it is again straightforward to numerically evaluate the integral in (4.32) and hence obtain $E_1(R)$ for the chosen values of R .

For the second excited state energy level $E_2(R)$, the situation is much more complicated. In this case there are two distinct regions of R defined respectively by the bounds $r < r_c$

⁵We examined a number of different R values in the range $10^{-4} < R < 10$.

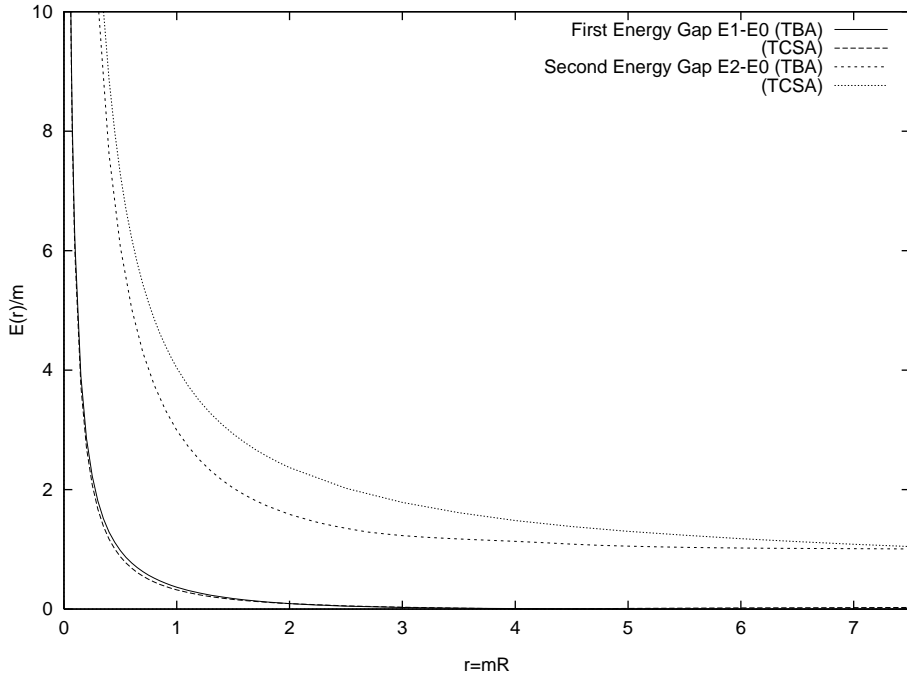


Figure 5: The two lowest energy level differences $E_1(R) - E_0(R)$ and $E_2(R) - E_1(R)$ obtained numerically from the TBA data shown in Figure 6.4 and presented respectively in Table 6.1 and 6.2, and from the TCSA method [13] described in Section 5.4.1.

and $r > r_c$, where the critical value r_c is specified by (4.10). In fact, these two regions are described by quite different energy expressions and TBA equations. For $r < r_c$, the energy level $E_2(R)$ is determined by the expression (4.41), which depends on the TBA equations (4.38) and the associated constraint condition (4.40). Similarly, for $r > r_c$ the energy level $E_2(R)$ is determined by the expression (4.46), which depends on the TBA equations (4.43) and the associated constraint condition (4.45). In both of these cases, accounting for the additional constraint equations as well as the convergence problems (which are similar in nature to those described above) present some extra difficulties for the numerical solution of the two sets of TBA equations. However, a more significant problem in this case is that all of the aforementioned numerical strategies breakdown in the region around the critical value r_c of the scaling parameter r . This problem is avoided here through the use of an interpolating function to describe the energy level $E_2(R)$ in the vicinity of the crossover between these two descriptions.

In Figure 4, the energy levels $E_0(R)$, $E_1(R)$ and $E_2(R)$ derived from the TBA methods outlined above, are plotted as functions of the scaling length $r = mR$. A comparison of these excited state TBA results can also be made with the known TCSA results [13]. In particular, it is most useful to compare the energy level differences $E_1(R) - E_0(R)$ and $E_2(R) - E_0(R)$ obtained

mR	$E_1 - E_0$ (TBA)	(TCSA)
0.00001	62831.56445476	62831.35411
0.000025	25132.45254369	25132.24227
0.00005	12566.08193960	12565.87166
0.000075	8377.291734939	8377.081465
0.0001	6282.896637100	6282.686370
0.00025	2512.985451883	2512.775232
0.0005	1256.348396107	1256.138248
0.00075	837.4693800061	837.2593044
0.001	628.0298740896	627.8198712
0.0025	251.0387832873	250.8292145
0.005	125.3751232181	125.1662761
0.0075	83.48726742289	83.27913960
0.01	62.54336272361	62.33595193
0.025	24.84453166641	24.64137450
0.05	12.27863838885	12.08239070
0.075	8.090337319392	7.900781170
0.1	5.996443118481	5.813368363
0.25	2.229783044794	2.081577717
0.5	0.9794797481711	0.876706700
0.75	0.5680114390827	0.498611616
1.0	0.3669407772837	0.321935555
2.5	0.05008836227296	0.0531794399
5.0	0.00286684507277	0.0101268211
7.5	0.00018876702243	0.0276849431

Table 1: A comparison of some numerical results for the lowest energy gap $E_1(R) - E_0(R)$ evaluated from the TBA approach using equations (4.25), (4.29), (4.31) and (4.32), and from the TCSA method [13] described in Section 5.4.1.

from both of these approaches. These energy level differences are plotted in Figure 5. Some particular values of these energy level differences are also presented in Tables 1 and 2. It is quite obvious from Figure 5 that the agreement between the TBA and TCSA results is extremely good for the first energy level difference, but is somewhat poorer for the second energy level difference (especially at intermediate values of r). A total agreement with TCSA is not really anticipated since the dimension of the perturbation in (2.1) $\Delta = 3/4$ exceeds the value $\Delta = 1/2$ above which the TCSA method requires modifications due to divergence problems. We refer the reader to [34] where these problems of the TCSA method are more thoroughly discussed.

mR	$E_2 - E_0$ (TBA)	(TCSA)
0.001	3141.370972547	3142.779881
0.002	1570.806398677	1571.982982
0.004	785.0624826259	786.5836788
0.006	523.2879477632	524.7831553
0.008	392.3470761712	393.8823300
0.01	313.9321721220	315.3413864
0.02	156.7885662688	158.2561799
0.04	78.24246832636	79.70552037
0.06	52.06938686002	53.51512707
0.08	38.99405029948	40.41507268
0.1	31.13990032524	32.55135753
0.2	15.44209616262	16.79944053
0.4	7.618391854072	8.876100399
0.6	5.028671954372	6.206070558
0.8	3.750083921383	4.856641130
1.0	2.994096980864	4.038850086
2.0	1.585738482126	2.367628184
2.5	1.352089391730	2.021744859
4.0	1.151471437505	1.482792705
5.0	1.053476286910	1.302407192
6.0	1.022056716644	1.178501191
7.5	1.006154507587	1.046907854

Table 2: A comparison of some numerical results for the second lowest energy gap $E_2(R) - E_0(R)$ evaluated from the TBA approach using equations (4.25), (4.29), (4.38), (4.40), (4.41), (4.43), (4.45) and (4.46), and from the TCSA method [13] described in Section 5.4.1.

5.2 Massless case

Consider now the asymptotic expansions of the operator $\mathbb{T}(\theta)$ at large values of θ . For simplicity restrict ourselves to the CFT case by replacing the $r \cosh(\theta)$ term in (4.17), (4.18) by $\frac{1}{2} r e^\theta$. The equation (4.17) can now be written as

$$e^{-\frac{r}{8}e^\theta} \frac{\mathbb{T}(\theta + i\pi/3)\mathbb{T}(\theta - i\pi/3)}{\mathbb{T}(\theta)} = 1 + \mathbb{Y}_0^{-1}(\theta) \quad (5.47)$$

The ground state eigenvalue $\mathbb{T}^{(0)}(\theta)$ of $\mathbb{T}(\theta)$ does not have zeroes in the strip $|\Im m \theta| < \pi/3$. Therefore, with an account of the asymptotics (4.16), the equation (5.47) implies

$$\log \mathbb{T}^{(0)}(\theta) = -\frac{\sqrt{3}r}{8\pi} \theta e^\theta + \mathbb{C}e^\theta + \phi * \log(1 + e^{-\epsilon_0(\theta)}) \quad (5.48)$$

where \mathbb{C} is an arbitrary constant and $\epsilon_0(\theta)$ determined by the ‘‘massless’’ version of (4.25) with the $r \cosh(\theta)$ term replaced by $\frac{1}{2} r e^\theta$.

Expanding the kernel (2.9) in a series

$$\phi(\theta) = -\frac{2}{\pi} \sum_{n=1}^{\infty} \sin \frac{2\pi(n+1)}{3} e^{(1-2n)\theta} . \quad (5.49)$$

one gets from (5.48)

$$\log \mathbb{T}^{(0)}(\theta) = -\frac{\sqrt{3}r}{8\pi} \theta e^\theta + \mathbb{C} e^\theta - \frac{2}{\pi} \sum_{n=1}^{\infty} \sin \frac{2\pi(n+1)}{3} \chi_n e^{(1-2n)\theta} . \quad (5.50)$$

where

$$\chi_n = \int_{-\infty}^{\infty} e^{(2n-1)\theta} (1 + e^{-\epsilon_0(\theta)}) d\theta \quad (5.51)$$

The numerical values of these coefficients can be compared with the the exact results of [11] where CFT's with extended \mathcal{W}_3 symmetry were studied. To facilitate this comparison let us introduce a new variable

$$t^2 = \frac{3re^\theta}{8\pi a^2} \quad (5.52)$$

where a is a normalisation constant and rewrite the first terms of the expansion (5.50) as

$$\mathbb{T}^{(0)}(t) = -\frac{2}{\sqrt{3}}(at)^2 \log t + \mathbb{C} t^2 - \frac{3\sqrt{3}}{2} (at)^{-2} I_1^{(0)} + \frac{32805\sqrt{3}}{43472} (at)^{-10} I_5^{(0)} + \dots \quad (5.53)$$

According to [11] the quantities $I_1^{(0)}$ and $I_5^{(0)}$ are the vacuum eigenvalues of the local integrals of motion in a particular highest weight module of the \mathcal{W}_3 algebra with the value of the central charge $c = 6/5$ (see [11] for further details). Their exact values [11]

$$I_1^{(0)} = -\frac{1}{20}, \quad I_5^{(0)} = -\frac{121}{10500} \quad (5.54)$$

are in good agreement with numerical values obtained from (5.51)

$$I_1^{(0)} = -0.499999999599 \cdot 10^{-1}, \quad I_5^{(0)} = -0.115238095240 \cdot 10^{-1} \quad (5.55)$$

Similar calculations for the first excited state of Sect. 4.2 in the ‘‘massless’’ limit give

$$I_1^{(1)} = 0.500000000002 \cdot 10^{-1}, \quad I_5^{(1)} = 0.497619047634 \cdot 10^{-2} \quad (5.56)$$

which again in a good agreement with the corresponding exact values of [11]

$$I_1^{(1)} = \frac{1}{20}, \quad I_5^{(1)} = \frac{209}{42000} \quad (5.57)$$

5.3 Functional Equations

Finally note, that the functional equation (4.1) can be obtained from the general set of of $A_2^{(2)}$ fusion relations [32]

$$\mathbf{T}_n\left(u + \lambda - \frac{\pi}{2}\right) \mathbf{T}_n\left(u - \lambda + \frac{\pi}{2}\right) = \mathbf{T}_{n-1}(u) \mathbf{T}_{n+1}(u) + f_{n+1}\left(u - \frac{3\lambda}{2}\right) \mathbf{T}_n\left(u + \frac{\pi}{2}\right) \quad (5.58)$$

where

$$\mathbf{T}_{-1}(u) \equiv 0, \quad \mathbf{T}_0 = (-1)^N f_0\left(u - \frac{3\lambda}{2}\right), \quad \mathbf{T}_1(u) \equiv \mathbf{T}(u), \quad (5.59)$$

$$f_n(u) = \left(p^{-\frac{1}{2}}\theta_1(u - v_n)\theta_1(u + v_n)\right)^N, \quad v_n = \frac{\pi}{4}((2n + 1)g + 1) \quad (5.60)$$

where the theta function $\theta_1(u) = \theta_1(u, p)$ defined in (A.1) and

$$g = 1 - \frac{2\lambda}{\pi} \quad (5.61)$$

We would like to stress that the relation (5.58) holds for arbitrary values of the parameters λ and ω in (3.5), where it can be considered just as a definition the “fused” transfer matrices $\mathbf{T}_n(u)$, $n \geq 2$, in terms of $\mathbf{T}_1(u) \equiv \mathbf{T}(u)$. The eigenvalue expression (3.5) and the Bethe Ansatz equations (3.8) ensure that all the higher transfer matrices $\mathbf{T}_n(u)$, $n \geq 2$, are entire functions of the variable u as well as $\mathbf{T}(u)$. For some special values of of the parameters λ and ω the infinite set of relation (5.58) truncates and becomes a system of functional equations for a finite number of the transfer matrices $\mathbf{T}_n(u)$. Let us a introduce a new variable

$$t = p^{-1}e^{2i(u-3\lambda/2)} \quad (5.62)$$

and rescale the transfer matrices as

$$\mathbf{T}_n(u) = (pt)^{-N}\mathbf{T}_n(t). \quad (5.63)$$

The relation (5.58) then becomes

$$\mathbf{T}_n(tq) \mathbf{T}_n(tq^{-1}) = \mathbf{T}_{n-1}(t) \mathbf{T}_{n+1}(t) + \phi_{n+1}(t) \mathbf{T}_n(-t) \quad (5.64)$$

with

$$q = e^{i\pi g} \quad (5.65)$$

and

$$\phi_n(t) = [\phi(itq^{n+\frac{1}{2}})\phi(-itq^{-n-\frac{1}{2}})]^N, \quad \phi(t) = \sum_{k=-\infty}^{\infty} (-1)^n p^{n^2} t^n \quad (5.66)$$

Now it is easy to see that if the the scalar factor $\phi_{n+1}(t)$ is omitted the relation (5.64) coincide with a particular case (corresponding to the $A_2^{(2)}$ reduction) of the more general $A_2^{(1)}$ fusion

relations considered in ref. [11] (see eqs.(5.14), (6.47), (6.48) therein). Note, that all reasonings of [11] can be modified to take into account the above scalar factor $\phi_{n+1}(t)$ in (5.64). Then using the determinant expressions (5.1), (5.2) of ref. [11] (see also the discussion in Sect.8.1 of that paper) one can show that if

$$q^{2(m+2)} = 1, \quad \text{and} \quad \omega^{m+2} = 1, \quad (5.67)$$

for some integer m then

$$\mathbf{T}_m(t) \equiv 0, \quad \mathbf{T}_{m-k-1}(t) = \mathbf{T}_k(-q^{m+2}t), \quad k = 0, 1, \dots, m-1. \quad (5.68)$$

The equation (4.1) corresponds to a particular case of this reduction

$$m = 4, \quad \lambda = \pi/12, \quad q = e^{5\pi i/6} \quad (5.69)$$

Another simple case is

$$m = 4, \quad \lambda = \pi/6, \quad q = e^{2\pi i/3}, \quad (5.70)$$

where (5.64) and (5.68) imply (assuming N even)

$$\mathbf{T}(tq^{\frac{1}{2}}) \mathbf{T}(tq^{-\frac{1}{2}}) = (\phi_0(-t) + \phi_2(-t)) \mathbf{T}(t) \quad (5.71)$$

The leading $p \rightarrow 0$ singularity of the free energy of the dilute A_2 lattice model of Sect.3 with this value of $\lambda = \pi/6$ is $\log k(u) \sim p^2 \log p \sin(2u)$, which determines to the value of the correlation length exponent $\nu = 1$. Therefore the scaling limit of the model corresponds to

$$N \rightarrow \infty, \quad p \rightarrow 0, \quad r = 4\sqrt{3}pN = \text{finite} \quad (5.72)$$

where the equation (5.71) becomes

$$\mathbf{T}\left(\theta + \frac{i\pi}{3}\right) \mathbf{T}\left(\theta - \frac{i\pi}{3}\right) = 2 \cosh\left(\frac{r}{2} \cosh(\theta)\right) \mathbf{T}(\theta) \quad (5.73)$$

with $\theta = \log t$. The massless version of this equation is related to a certain $c = -2$ CFT with extended \mathcal{W}_3 symmetry [11] (Sect.6.3.2 therein).

Acknowledgements

The authors are grateful to S. O. Warnaar and P. Pearce for interesting discussions.

Appendix A

The Boltzmann weights of the off-critical dilute- A_M models are given by [18, 27]

$$\begin{aligned}
W\left(\begin{array}{cc|c} a & a & u \\ a & a & \end{array}\right) &= \rho \frac{\vartheta_1(6\lambda-u)\vartheta_1(3\lambda+u)}{\vartheta_1(6\lambda)\vartheta_1(3\lambda)} \\
&\quad - \rho \left(\frac{S(a+1)}{S(a)} \frac{\vartheta_4(2a\lambda-5\lambda)}{\vartheta_4(2a\lambda+\lambda)} + \frac{S(a-1)}{S(a)} \frac{\vartheta_4(2a\lambda+5\lambda)}{\vartheta_4(2a\lambda-\lambda)} \right) \frac{\vartheta_1(u)\vartheta_1(3\lambda-u)}{\vartheta_1(6\lambda)\vartheta_1(3\lambda)} \\
W\left(\begin{array}{cc|c} a \pm 1 & a & u \\ a & a & \end{array}\right) &= W\left(\begin{array}{cc|c} a & a & u \\ a & a \pm 1 & \end{array}\right) = \rho \frac{\vartheta_1(3\lambda-u)\vartheta_4(\pm 2a\lambda+\lambda-u)}{\vartheta_1(3\lambda)\vartheta_4(\pm 2a\lambda+\lambda)} \\
W\left(\begin{array}{cc|c} a & a & u \\ a \pm 1 & a & \end{array}\right) &= W\left(\begin{array}{cc|c} a & a \pm 1 & u \\ a & a & \end{array}\right) = \rho \left(\frac{S(a\pm 1)}{S(a)} \right)^{1/2} \frac{\vartheta_1(u)\vartheta_4(\pm 2a\lambda-2\lambda+u)}{\vartheta_1(3\lambda)\vartheta_4(\pm 2a\lambda+\lambda)} \\
W\left(\begin{array}{cc|c} a & a \pm 1 & u \\ a & a \pm 1 & \end{array}\right) &= W\left(\begin{array}{cc|c} a \pm 1 & a \pm 1 & u \\ a & a & \end{array}\right) = \\
&= \rho \left(\frac{\vartheta_4(\pm 2a\lambda+3\lambda)\vartheta_4(\pm 2a\lambda-\lambda)}{\vartheta_4^2(\pm 2a\lambda+\lambda)} \right)^{1/2} \frac{\vartheta_1(u)\vartheta_1(3\lambda-u)}{\vartheta_1(2\lambda)\vartheta_1(3\lambda)} \\
W\left(\begin{array}{cc|c} a \pm 1 & a & u \\ a & a \mp 1 & \end{array}\right) &= \rho \frac{\vartheta_1(2\lambda-u)\vartheta_1(3\lambda-u)}{\vartheta_1(2\lambda)\vartheta_1(3\lambda)} \\
W\left(\begin{array}{cc|c} a & a \mp 1 & u \\ a \pm 1 & a & \end{array}\right) &= -\rho \left(\frac{S(a-1)S(a+1)}{S^2(a)} \right)^{1/2} \frac{\vartheta_1(u)\vartheta_1(\lambda-u)}{\vartheta_1(2\lambda)\vartheta_1(3\lambda)} \\
W\left(\begin{array}{cc|c} a & a \pm 1 & u \\ a \pm 1 & a & \end{array}\right) &= \rho \frac{\vartheta_1(3\lambda-u)\vartheta_1(\pm 4a\lambda+2\lambda+u)}{\vartheta_1(3\lambda)\vartheta_1(\pm 4a\lambda+2\lambda)} + \rho \frac{S(a\pm 1)}{S(a)} \frac{\vartheta_1(u)\vartheta_1(\pm 4a\lambda-\lambda+u)}{\vartheta_1(3\lambda)\vartheta_1(\pm 4a\lambda+2\lambda)} \\
&= \rho \frac{\vartheta_1(3\lambda+u)\vartheta_1(\pm 4a\lambda-4\lambda+u)}{\vartheta_1(3\lambda)\vartheta_1(\pm 4a\lambda-4\lambda)} \\
&\quad + \rho \left(\frac{S(a\mp 1)}{S(a)} \frac{\vartheta_1(4\lambda)}{\vartheta_1(2\lambda)} - \frac{\vartheta_4(\pm 2a\lambda-5\lambda)}{\vartheta_4(\pm 2a\lambda+\lambda)} \right) \frac{\vartheta_1(u)\vartheta_1(\pm 4a\lambda-\lambda+u)}{\vartheta_1(3\lambda)\vartheta_1(\pm 4a\lambda-4\lambda)} \\
S(a) &= (-)^a \frac{\vartheta_1(4a\lambda)}{\vartheta_4(2a\lambda)} \\
\rho &= h(2\lambda)h(3\lambda).
\end{aligned}$$

The standard elliptic functions of variable u and nome $p = e^{-\tau}$ are defined as

$$\vartheta_1(u) \equiv \vartheta_1(u; p) = 2 \sum_{n=0}^{\infty} (-1)^n p^{(2n+1)^2/4} \sin[(2n+1)u] \quad (\text{A.1})$$

$$\vartheta_4(u) \equiv \vartheta_4(u; p) = 1 + 2 \sum_{n=1}^{\infty} (-1)^n p^{n^2} \cos(2nu). \quad (\text{A.2})$$

These have the useful (quasi-) periodicity properties

$$\vartheta_1(u+\pi; p) = -\vartheta_1(u; p), \quad \vartheta_1(u+i\tau; p) = -p^{-1}e^{-2iu}\vartheta_1(u; p) \quad (\text{A.3})$$

and

$$\vartheta_4(u+\pi, p) = \vartheta_4(u, p), \quad \vartheta_4(u+i\tau, p) = -p^{-1}e^{-2iu}\vartheta_4(u, p). \quad (\text{A.4})$$

References

- [1] V. V. Bazhanov, S. L. Lukyanov, and A. B. Zamolodchikov: Integrable Quantum Field Theories in Finite Volume: Excited State Energies, *Nucl. Phys.* **B489** (1997), 487-531.
- [2] P. Dorey, and R. Tateo: Excited States by Analytic Continuation of TBA Equations, *Nucl. Phys.* **B482** (1996), 639-659.
- [3] D. Fioravanti, A. Mariottini, E. Quattrini, and F. Ravanini: Excited State Destri-De Vega Equation for Sine-Gordon and Restricted Sine-Gordon Models, *Phys. Lett.* **B390** (1997), 243-152.
- [4] C. Destri, H.J. de Vega: Non Linear Integral Equation and Excited–States Scaling Functions in the Sine-Gordon Model, *Nucl. Phys.* **B504** (1997), 621-664.
- [5] P. Dorey, R. Tateo: Excited States in Some Simple Perturbed Conformal Field Theories, *Nucl. Phys.* **B515** (1998), 575-623.
- [6] P. Fendley: Excited-State Energies and Supersymmetric Indices, *Adv. Theor. Math. Phys.* **1** (1997), 210-236.
- [7] V. V. Bazhanov, S. L. Lukyanov, and A. B. Zamolodchikov: Integrable Structure of Conformal Field Theory, Quantum KdV Theory and Thermodynamic Bethe Ansatz, *Commun. Math. Phys.* **177** (1996), 381-398.
- [8] A. Klümper, and P. Pearce: Analytic Calculation of Scaling Dimensions: Tricritical Hard Squares and Critical Hard Hexagons, *J. Stat. Phys.* **64** (1991), 13-76.
- [9] A. Klümper, and P. Pearce: Conformal Weights of RSOS Lattice Models and Their Fusion Hierarchies, *Physica* **A183** (1992), 304-350.
- [10] D. Fioravanti, F. Ravanini, and M. Stanishkov: Generalised KdV and Quantum Inverse Scattering Description of Conformal Minimal Models, *Phys. Lett.* **B367** (1996), 113-120.

- [11] V.V. Bazhanov, A.N. Hibberd, S.M. Khoroshkin: Integrable structure of \mathcal{W}_3 Conformal Field Theory, Quantum Boussinesq Theory and Boundary Affine Toda Theory, *Nucl. Phys.* **B622** (2002), 475-547.
- [12] F. A. Smirnov: Exact S-Matrices for $\phi_{1,2}$ -Perturbed Minimal Models of Conformal Field Theory, *Int. J. Mod. Phys.* **A6** (1991), 1407-1428.
- [13] G. Mussardo: Integrable Deformations of the Nonunitary Minimal Conformal Model $\mathcal{M}_{3,5}$, *Int. J. Mod. Phys.* **A7** (1992), 5027-5044.
- [14] V. P. Yurov, and Al. B. Zamolodchikov: Truncated Conformal Space Approach to Scaling Lee-Yang Model, *Int. J. Mod. Phys.* **A5** (1990), 3221-3245.; V. P. Yurov, and Al. B. Zamolodchikov: Truncated-Fermionic-Space Approach to the Critical 2D Ising Model with Magnetic Field, *Int. J. Mod. Phys.* **A6** (1991), 4557-4578.
- [15] F. Ravanini, M. Stanishkov, and R. Tateo: Integrable Perturbations of CFT with Complex Parameter: The $\mathcal{M}_{3/5}$ Model and its Generalizations, *Int. J. Mod. Phys.* **A11** (1996), 677-697.
- [16] R. M. Ellem, and V. V. Bazhanov: Thermodynamic Bethe Ansatz for the subleading magnetic perturbation of the tricritical Ising Model, *Nucl. Phys.* **B512** (1998), 563-580.
- [17] V. V. Bazhanov, S. L. Lukyanov, and A. B. Zamolodchikov: Integrable Structure of Conformal Field Theory II: Q-operator and DDV equation, *Commun. Math. Phys.* **190** (1997), 247-278.
- [18] S. O. Warnaar, B. Nienhuis, and K. A. Seaton: New Construction of Solvable Lattice Models Including an Ising Model in a Magnetic Field, *Phys. Rev. Lett.* **69** (1992), 710-.; S. O. Warnaar, B. Nienhuis, and K. A. Seaton: A Critical Ising Model in a Magnetic Field, *Int. J. Mod. Phys.* **B7** (1993), 3727-3736.
- [19] C. N. Yang, and C. P. Yang: Thermodynamics of a One-Dimensional System of Bosons with Repulsive Delta-Function Interaction, *J. Math. Phys.* **10** (1969), 1115-1122.
- [20] Al. B. Zamolodchikov: Thermodynamic Bethe Ansatz for RSOS Scattering Theories, *Nucl. Phys.* **B358** (1991), 497-523.
- [21] A. B. Zamolodchikov: Integrals of Motion in Scaling 3-State Potts Model Field Theory, *Int. J. Mod. Phys.* **A3** (1988), 743-750.; A. B. Zamolodchikov: Integrable Field Theory from Conformal Field Theory, *Advanced Studies in Pure Mathematics* **19** (1989), 641-674.; A.

- B. Zamolodchikov: Integrals of Motion and S -Matrix of the (Scaled) $T = T_c$ Ising Model with a Magnetic Field, *Int. J. Mod. Phys.* **A4** (1989), 4235-4248.
- [22] V. A. Fateev: The Exact Relations between the Coupling Constants and the Masses of Particles for the Integrable Perturbed Conformal Field Theories, *Phys. Lett.* **B324** (1994), 45-51.
- [23] R. J. Baxter: Hard Hexagons: Exact solution, *J. Phys.* **A13** (1980), L61-L70.
- [24] V. V. Bazhanov, and N. Yu. Reshetikhin: Critical RSOS Models and Conformal Field Theory, *Int. J. Mod. Phys.* **A4** (1989), 115-142.
- [25] C. N. Yang: Some Exact Results for the Many-Body Problem in One Dimension with Repulsive Delta-Function Interaction, *Phys. Rev. Lett.* **19** (1967), 1312-1315.
- [26] V. M. Filyov, A. M. Tsvelick, and P. B. Wiegmann: Thermodynamics of the s - d Exchange Model (Kondo Problem), *Phys. Lett.* **A81** (1981), 175-178.; A. M. Tsvelick, and P. B. Wiegmann: Exact results in the theory of Magnetic Alloys, *Advances in Physics* **32** (1983), 453-713.
- [27] S. O. Warnaar, P. A. Pearce, K. A. Seaton, and B. Nienhuis: Order Parameters of the Dilute A Models, *J. Stat. Phys.* **74** (1994), 469-531.
- [28] V. V. Bazhanov, B. Nienhuis, and S. O. Warnaar: Lattice Ising Model in a Field: E_8 Scattering Theory, *Phys. Lett.* **B322** (1994), 198-206.
- [29] M. Takahashi, and M. Suzuki: One-Dimensional Anisotropic Heisenberg Model at Finite Temperature, *Prog. Theor. Phys.* **48** (1972), 2187-2209.
- [30] Y. -K. Zhou, P. A. Pearce, and U. Grimm: Fusion of Dilute A_L Lattice Models, *Physica* **A222** (1995), 261-306.
- [31] Y. -K. Zhou: $SU(2)$ Hierarchies of Dilute Lattice Models, *Int. J. Mod. Phys.* **B10** (1996), 3481-3503.
- [32] A. Kuniba, and J. Suzuki: Functional Relations and Analytic Bethe Ansatz for Twisted Quantum Affine Algebras, *J. Phys.* **A28** (1995), 711-722.
- [33] A. Kuniba, and T. Nakanishi: Spectra in Conformal Field Theories from the Rogers Dilogarithm, *Mod. Phys. Lett.* **A7** (1992), 3487-3494.; A. Kuniba, and T. Nakanishi: Rogers Dilogarithm in Integrable Systems, in C. N. Yang, M. L. Ge, and X. W. Zhou (Eds.):

Proceedings of the XXI International Conference on Differential Geometric Methods in Theoretical Physics (Tianjin, China, 5-9th June 1992), World Scientific, Singapore, 1993.

- [34] M. Lässig, G. Mussardo, and J. L. Cardy: The Scaling Region of the Tricritical Ising Model in Two Dimensions, *Nucl. Phys.* **B348** (1991), 591-618.